Citation: Cell Death and Disease (2010) 1, e41; doi:10.1038/cddis.2010.16

www.nature.com/cddis

p53-mediated delayed NF-κB activity enhances etoposide-induced cell death in medulloblastoma

D Meley[1], DG Spiller[1], MRH White[1], H McDowell[2], B Pizer[2] and V Sée*[,1]

Medulloblastoma (MB) is an embryonic brain tumour that arises in the cerebellum. Using several MB cell lines, we have demonstrated that the chemotherapeutic drug etoposide induces a p53- and caspase-dependent cell death. We have observed an additional caspase-independent cell death mechanism involving delayed nuclear factor κB (NF-κB) activity. The delayed induction was controlled by a p53-dependent transcription step and the production of death receptors (especially CD95/Fas). We further demonstrated that in both MB and glioblastoma (GM) cell lines, in which the p53 pathway was not functional, no p65 activation could be detected upon etoposide treatment. MB cell lines that have mutations in p53 or NF-κB are either less sensitive (NF-κB mutant) or even completely resistant (p53 mutant) to chemotherapeutic intervention. The optimal cell death was only achieved when both p53 and NF-κB were switched on. Taken together, our results shed light on the mechanism of NF-κB activation by etoposide in brain tumours and show that the genetic background of MB and GM cells determines their sensitivity to chemotherapy and has to be taken into account for efficient therapeutic intervention.
Cell Death and Disease (2010) **1,** e41; doi:10.1038/cddis.2010.16; published online 13 May 2010
Subject Category: Cancer

Medulloblastoma (MB) is the most common malignant brain tumour in children.[1] It is a primitive neuro-ectodermal tumour, arising from neural stem cell precursors in the granular cell layer of the cerebellum. Current treatments include different combinations of surgical resection, craniospinal radiotherapy and chemotherapy. The survival rate as a function of the tumour stage is between 60 and 80%. However, despite the efficiency of current treatments, survivors still suffer significant long-term after-effects and children younger than 3 years old have a less favourable prognosis as some therapy modalities are not possible.[2] Etoposide is one of the currently used clinical chemotherapeutic agents. It damages DNA by stabilising the DNA-topoisomerase II complex, thus increasing the frequency of double-stranded DNA breaks. However, tumours display different sensitivities to this drug and the molecular mechanisms of resistance are largely unknown. Etoposide has previously been shown to activate the proinflammatory nuclear factor κB (NF-κB)-dependent signalling pathway,[3,4] the tumour suppressor p53 transcription factor,[5] as well as the death receptor (DR) Fas expression.[6] NF-κB is a family of transcription factors; RelA/p65, the main member of the canonical pathway is involved in inflammation,[7] cell cycle progression[8] and tumorigenesis.[9] Yet the effects of its activity are blurred because of its dual role as a pro- or antiapoptotic factor.[10] Its role in cell death has previously been reported in several cellular models including neuroblastoma.[11,12] p53 responds to DNA damage or deregulation of mitogenic oncogenes through the induction of cell cycle arrest, apoptosis or cellular senescence. Mutations in p53 are often associated with aggressive tumour behaviour and poor patient prognosis.[13]

Previous investigations have indicated potential crosslink between p53 and NF-κB pathways, but relatively few studies explore the molecular mechanisms involved. The best described mechanisms of crosstalk are (1) direct competitive interaction between p53 or p65 with the transcriptional coactivator proteins p300 and CREB-binding protein (CBP),[14–16] and (2) the recruitment of the non-canonical NF-κB member p52 by p53 and subsequent regulation of p53-dependent genes.[17] We demonstrate here, for the first time, a new molecular bridge between NF-κB and p53 that involves transcription and expression of DRs. The DR family includes Fas (CD95/APO-1), death receptor 3–6 (DR3–6) and tumour necrosis factor-R1 (TNF-R1) receptors. A shared feature of DRs is a conserved 80 amino-acid sequence, the death domain, in the cytoplasmic tail of these molecules.

[1]Centre for Cell Imaging, School of Biological Sciences, University of Liverpool, Liverpool L69 7ZB, UK and [2]Alder Hey Children's NHS Foundation Trust, Liverpool L12 2AP, UK
*Corresponding author: V Sée, Centre for Cell Imaging, School of Biological Sciences, University of Liverpool, Liverpool L69 7ZB, UK.
Tel: +44 151 795 4598; Fax: +44 151 795 4404; E-mail: violaine@liverpool.ac.uk
Keywords: medulloblastoma; glioblastoma; NF-κB; p53; CD95/Fas; DNA damaging agents
Abbreviations: CBP, CREB-binding protein; DR3–6, death receptor 3–6; EGFP, enhanced green fluorescent protein; FADD, Fas-associated via death domain; FasL, Fas ligand; GM, gliobastoma; IκBα, inhibitor of nuclear factor κBα; IKK, IκB Kinase; MB, medulloblastoma; mdm2, mouse double minute 2; NF-κB, nuclear factor κB; PFTα, pifithrin-α; TNFα, tumour necrosis factor-α
Received 26.10.09; revised 22.3.10; accepted 26.3.10; Edited by A Verkhrasky

Upon activation of Fas, sequential association of the adaptor molecule Fas-associated via death domain (FADD) and pro-forms of caspase 8 lead to the death signalling.[18]

We have observed a delay in p65 activation following etoposide treatment compared with the classical TNFα activator, due to an essential transcription/translation mechanism. We have further identified p53 and Fas as key mediators of this activity in MB cells. We have used different MB cell lines (D283-MED, MHH-Med1, MEB-Med8A and D458-MED cells) that bear differential mutation status in the NF-κB and/or p53 genes, and showed that they are correlated to differential sensitivity to chemotherapeutic treatment. Similar results were obtained in some glioblastoma (GM) cell lines (D566-MG, U87MG and T98G cells). Altogether our data strongly suggest a clear molecular mechanism for etoposide-induced cell death in brain tumours, which ought to be taken into account to maximise the efficiency of clinical management.

Results

Etoposide induces a delayed p65 activation in MB cells. Etoposide has previously been shown to activate p65.[3,19] We have probed this activation in MB cells by western blot with an anti-phospho-Ser536 p65 antibody. We observed p65 phosphorylation 6 h after etoposide treatment in D283-MED and D458-MED cells. Interestingly, this phosphorylation was not observed in MHH-Med1 or in MEB-Med8A cell lines (Figure 1a). This phosphorylation event was further correlated with p65-dependent transcription. Using luminometry, we have shown that only D283-MED and D458-MED cells displayed an etoposide-induced NF-κB-dependent transcriptional activity (Figure 1b). As a positive control, TNFα was used to show that NF-κB could be induced in these cells. It was found that MHH-Med1 cells did not respond to TNFα, but all of the other three cell lines showed the expected NF-κB response (Figure 1d and e and Supplementary Figure S1A–C). Despite the observation that Ser536 phosphorylation is essential for p65 activity, we further analysed the absence of NF-κB induction upon TNFα treatment in MHH-Med1 cells. We showed that 10 ng/ml of TNFα was unable to induce inhibitor of nuclear factor κBα (IκBα) degradation, p65 nuclear translocation and NF-κB-dependent transcription (Supplementary Figure S1D–F).

We then used the D283-MED cells as a model cell line and probed the role of IκB Kinases (IKKs) and IκBα in etoposide-induced p65 phosphorylation. Treatment of D283-MED cells with the IKKs inhibitor BMS-345541 or IκBα inhibitor Bay11-7082 inhibited etoposide-induced p65 phosphorylation (Figure 1c), showing the essential function of IKKα/β and IκBα in etoposide-induced p65 signalling. The dynamics of p65 activation and translocation into the nucleus were also examined using time-lapse confocal microscopy of single living cells transfected with vectors encoding p65-RedXP and IκBα-enhanced green fluorescent protein (EGFP) fluorescent fusion proteins (Figure 1d). As previously demonstrated in other cell lines,[4,20] we observed damped p65 nuclear-cytoplasmic oscillations after TNFα treatment. The first peak of nuclear occupancy was at ~60 min after TNFα treatment. Following etoposide treatment, p65 translocation into the nucleus was delayed by 1 h and the peak amplitude was reduced (Figure 1d). The delay in p65 activation was confirmed by western blotting (Supplementary Figure S1A) and by luminescence imaging (Figure 1e) using a NF-luciferase reporter vector containing 5 repeats of NF-κB-binding sites cloned upstream of the luciferase gene. The presence of a delay suggested that p65 activation might be indirect. To determine if the delay was caused by an earlier transcriptional and/or translational event, we inhibited transcription with actinomycin-D (Figure 1f) or translation with cycloheximide (Supplementary Figure S2) 30 min before TNFα/etoposide treatment. Etoposide-induced p65 phosphorylation was prevented by both inhibitors, suggesting that a first transcription/translation event was essential for etoposide-induced p65 activation. As expected, the inhibition of transcription/translation did not affect TNFα-induced p65 phosphorylation.

Medulloblastoma cell lines displayed different sensitivity to etoposide involving both caspase-dependent and -independent programmes. The effect of etoposide on cell viability in different MB cell lines was assessed using the 3-(4, 5-dimethylthiazol-2-yl)-5-(3-carboxymethoxyphenyl)-2-(4-sulfophenyl)-2H-tetrazolium (MTS) assay (Figure 2a). This showed that these cell lines displayed a different sensitivity to etoposide treatment. We observed ~80% of cell death 24 h after treatment in both D283-MED and D458-MED cells, whereas MHH-Med1 displayed only 58% of death at the same time. Conversely, MEB-Med8A cells were strongly resistant to etoposide treatment up to 24 h. We next investigated the role of p65 activity in the cell death programme activated by etoposide. Inhibition of NF-κB pathway in D283-MED cells was obtained either with various NF-κB inhibitors (Wedelolactone: IKK complex inhibitor; Bay11-7082: IκBα inhibitor; JSH-23: p65 nuclear translocation inhibitor) or by using p65 siRNA. This inhibition partially or totally prevented etoposide-induced cell death (Figure 2b and c), suggesting a key role for NF-κB in etoposide-induced cell death in these cells. Similar results were obtained for D458-MED cells (not shown). In contrast, MHH-Med1 cells (in which no p65 activity could be detected) were not protected by NF-κB inhibition (Supplementary Figure S3A).

To further characterise the type of cell death induced by etoposide, we measured the caspase 3/7 activity in each cell line (Figure 2d). In accordance with the viability assay, we observed strong and fast caspase-3 activation in D283-MED and D458-MED cells; however, no caspase-3 activation could be observed in MEB-Med8A until 24 h after etoposide treatment. This was in line with the resistance of this cell line to etoposide-induced cell death. Surprisingly, MHH-Med1 cells displayed a stronger caspase activity compared with D283- and D458-MED cells, although lower cell death was observed in these cells (Figure 2a and d). This suggests the involvement of a different cell death mechanism, which was independent of caspase-3 activation. Evidence to support this hypothesis was that blocking NF-κB activity with Bay11-7082 did not prevent caspase-8 or 3/7 induction (Figure 2e), but

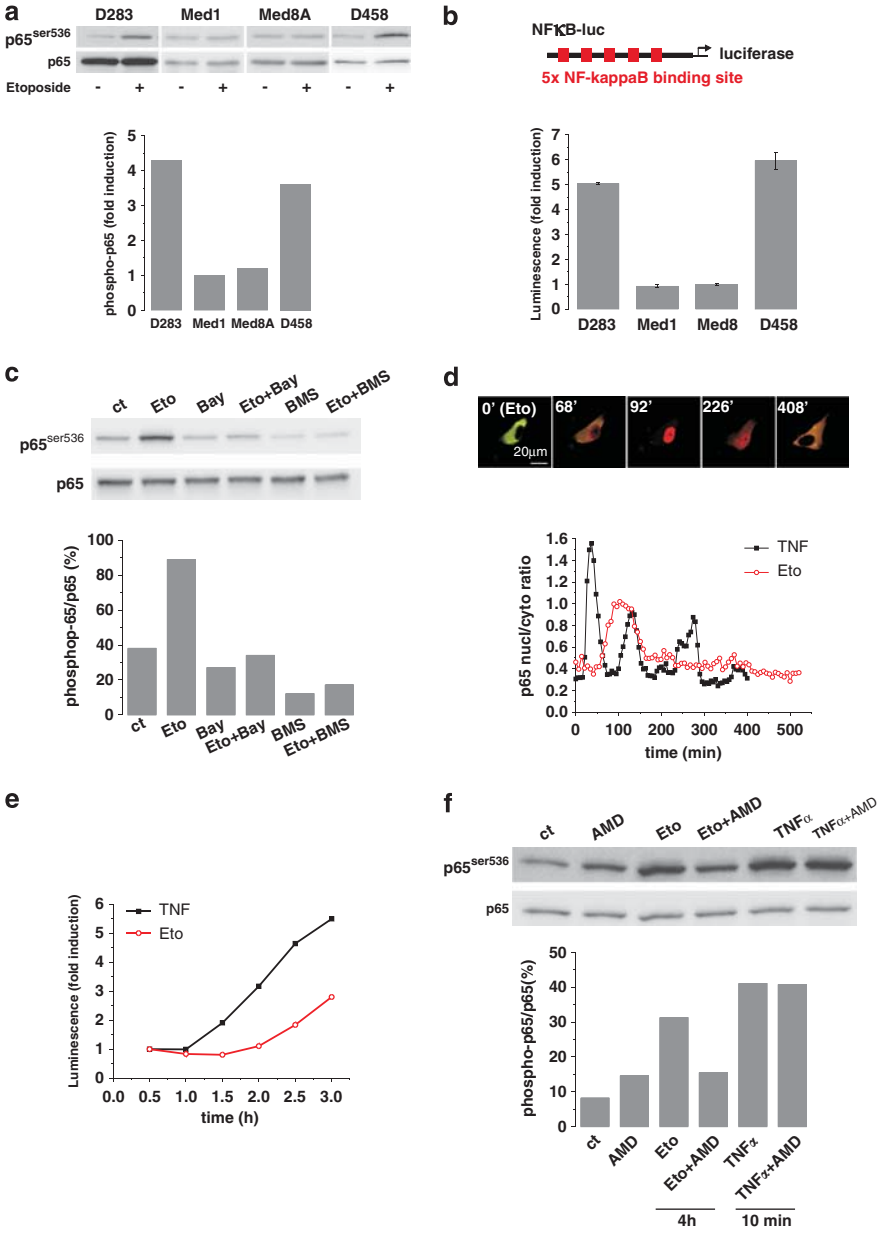

Figure 1 Etoposide induces a delayed p65 activation in some MB cells. (**a**) Four MB cell lines were treated with 20 μM etoposide for 6 h. p65 and p65-Ser536 phosphorylation levels were assessed by western blot. The blot presented is representative of three independent experiments. Quantification of the bands was plotted as p65 phosphorylation fold increase compared with the control non-treated cells. (**b**) After 24 h transfection with NF-luc plasmid, cells were treated with 20 μM etoposide for 8 h before assessment of the luciferase activity. Relative luminescence measurements to t0 are plotted for each cell line. (**c**) D283-MED cells were simultaneously treated for 6 h with 20 μM etoposide and 5 μM Bay11-7082 or 10 μM BMS-345541. p65 phosphorylation was analysed by western blot. The blot presented is representative of three independent experiments and the plot represents the quantification of the blot shown. (**d**) D283-MED cells transfected with p65-RedXP and IκBα-EGFP were treated with 20 μM etoposide or 10 ng/ml TNFα. Time-lapse confocal microscopy was performed as described in Materials and Methods. Mean fluorescence intensities for individual cells were analysed. A typical cell for each treatment was plotted as the p65 nuclear/cytoplasmic ratio as a function of time. (**e**) D283-MED cells transfected with NF-Luc vector were treated with 20 μM etoposide or 10 ng/ml TNFα. Real-time luminescence signal was captured as described in Materials and Methods. The graph represents mean luminescence intensities measured in whole field. (**f**) D283-MED cells were pretreated 30 min with 5 μg/ml of the transcription inhibitor actinomycin-D, prior to a 10 min treatment with 10 ng/ml TNFα, or a 4 h treatment with 20 μM etoposide. p65 phosphorylation levels were analysed by western blot. The blot presented is representative of three independent experiments and the plot represents the quantification of the blot shown

protected the cells from etoposide cytotoxicity (Figure 2b). These data suggest that p65 may be involved in a caspase-independent cell death pathway that may enhance another form of etoposide-induced caspase-dependent cell death. Etoposide-induced cell death was further characterised by an annexin V–propidium iodide assay and we observed by flow cytometry both apoptosis and necrosis (not shown). An assay of macroautophagy induction by acidic vacuoles staining with the monodansylcadaverine dye suggested some autophagy induction (Supplementary Figure S4).

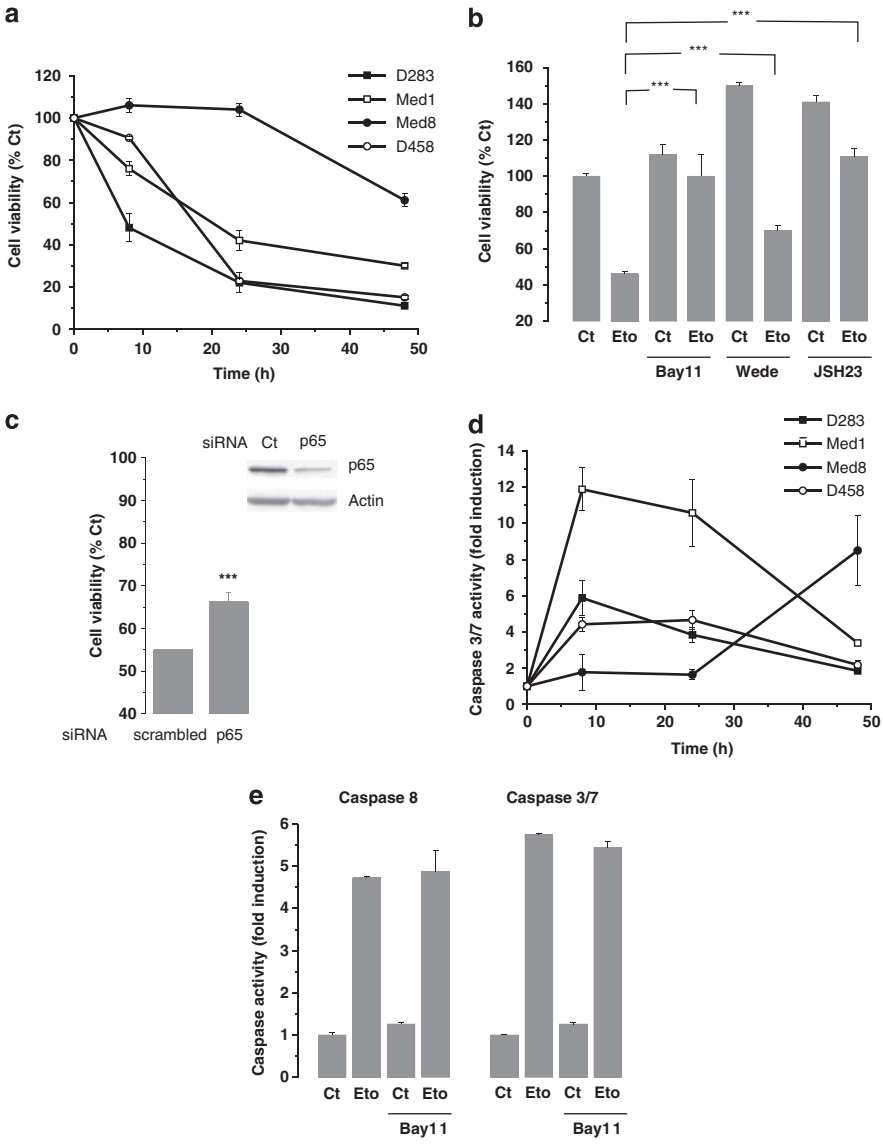

Figure 2 MB cell lines displayed different sensitivity to etoposide involving both caspase-dependent and -independent cell death. (**a**) Cell viability was analysed by MTS assay at indicated time points, upon 20 μM etoposide treatment. (**b**) Viability of D283-MED cells treated with 20 μM etoposide in the presence of 5 μM Bay11-7082, 10 μM Wedelolactone or 5 μM JSH23 was assessed by MTS assay. (**c**) D283-Med cells were transfected with 100 nM of siRNA directed against p65 or a control scrambled siRNA. After 48 h, cells were treated with 20 μM etoposide for 8 h and viability was assessed by MTS assay. The knockdown efficiency was controlled by western blot (insert). (**d**) Several MB cell lines were treated with 20 μM etoposide for indicated times. Caspase 3/7 activity was measured with Caspase-Glo 3/7 assay kit. Results are expressed as fold-induction compared with control non-treated cells as a function of time. (**e**) D283-MED cells were treated with 20 μM etoposide in presence or absence of 5 μM Bay11-7082 for 8 h. Caspase 8 and 3/7 activities were assessed with Caspase-Glo assay kits. Results are relative to control non-treated cells. **a–d** results are the mean of three independent experiments ± S.E.M. '***' indicates statistical difference with $P<0.001$

p53 is required for etoposide-induced p65 activity in MB cells. We have shown that transcription and translation were required for delayed p65 activation and subsequent NF-κB-dependent death (Figure 1f and Supplementary Figure S2). As etoposide causes DNA damage, an obvious candidate intermediate is p53, the main DNA damage sensor. Previous work in neuroepithelial cells had suggested that etoposide induces cell death in p53-dependent manner.[21] Indeed, etoposide treatment induced an accumulation of p53 protein in D283-MED, D458-MED and MHH-Med1 cells (Figure 3a). However, MEB-Med8A cells expressed a low level of p53wt, but a p53 isoform or truncated form was detected by Western blot with an additional band being evident at a slightly lower molecular weight. The accumulation of p53 in the three other cell lines was further correlated with the induction of p53-dependent transcription as shown by quantitative RT-PCR (qPCR) detection of the mouse double minute 2 (mdm2) transcripts (Figure 3b). We then investigated if p53 could be the upstream factor involved in the delayed p65 activation. Both invalidation of p53 expression using siRNA and treatment of D283-MED cells with Pifithrin-α (PFTα), a well-described p53 inhibitor,

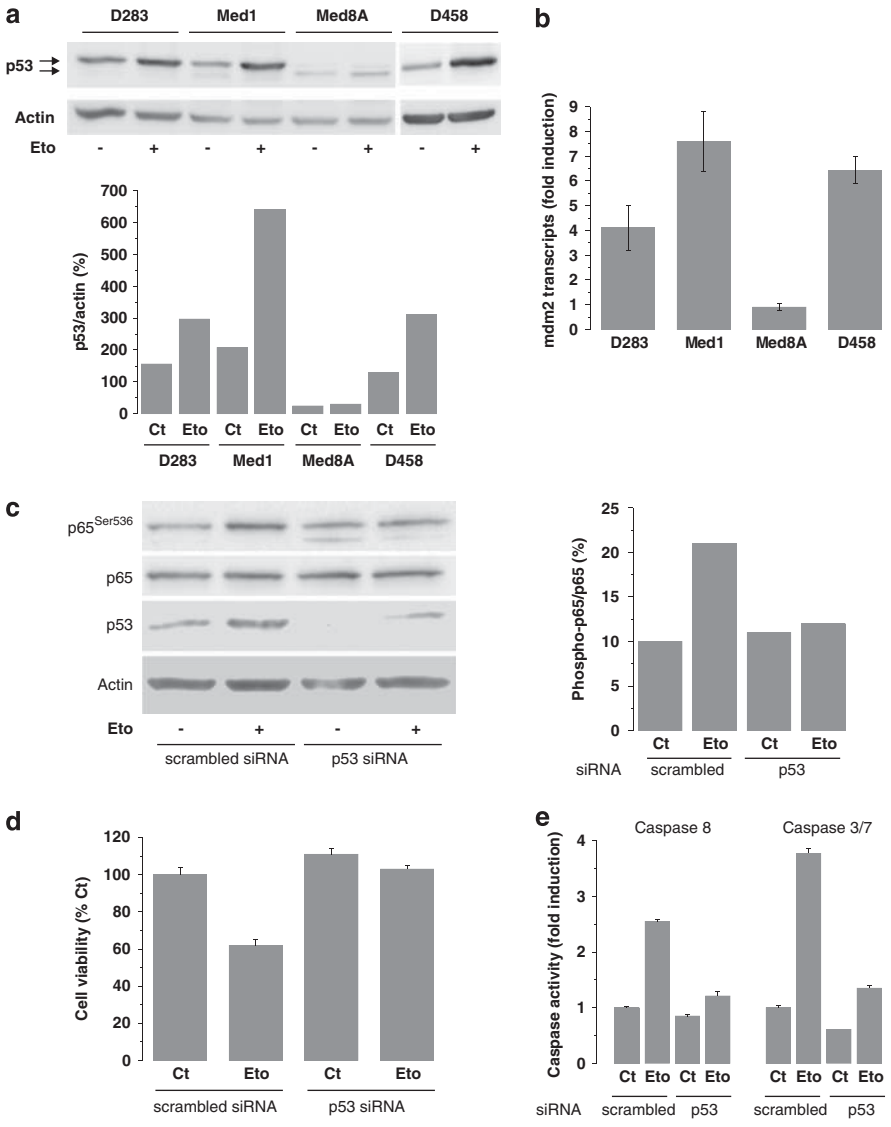

Figure 3 Etoposide-induced p65 activation is p53 dependent in MB cells. (**a**) Cells were treated with 20 μM etoposide for 6 h and p53 expression levels were measured by western blot in different MB cell lines. The blot presented is representative of three independent experiments and the plot represents the quantification of the blot shown. (**b**) qPCR relative quantification of mdm2 mRNA expression in all cell lines was assessed upon 8 h of etoposide treatment (20 μM). The plot represents the relative fold induction compared to control non-treated cells. (**c**–**e**) D283-MED cells were transfected with 100 nM of siRNA directed against p53 or a control-scrambled siRNA for 48 h before etoposide treatment. The efficiency of the knockdown is shown on the blot in panel c. (**c**) Cells were treated with 20 μM etoposide for 6 h. p65 phosphorylation levels were analysed by western blot. The blot presented is representative of three independent experiments and the plot represents the quantification of the blot shown. (**d**) Cells were treated with 20 μM etoposide for 8 h and viability was assessed using MTS assay. (**e**) Cells were treated with etoposide (20 μM, 8 h) and caspase activity was measured using Caspase-Glo 8 and 3/7 assay kits. Results are relative to control non-treated cells

strongly inhibited etoposide-induced p65 phosphorylation (Figure 3c and Supplementary Figure S5). Moreover, although the NF-κB pathway responded normally to TNFα in MEB-Med8A cells (Supplementary Figure S1C), the absence of etoposide-mediated p65 phosphorylation (Figure 1a) was most likely due to the absence of p53wt (Figure 3a) in these cells. We then demonstrated the role of p53 in etoposide-mediated cell death and in caspase activation. Invalidation of p53 expression using siRNA totally protected D283-MED cells (Figure 3d) and MHH-Med1 cells (Supplementary Figure S3B) to drug cytotoxicity and significantly inhibited caspases 8 and 3/7 activities (Figure 3e and Supplementary Figure S3C). These results indicated that p53 induction was a prerequisite for two distinct death pathways triggered by etoposide: one that was caspase-dependent and the other that was p65-dependent but caspase-independent.

The expression of Fas DR is required for p65 phosphorylation. To further elucidate the link between p53-dependent transcription and p65 activity, we have screened by qPCR several p53-dependent genes upon 6 h of etoposide treatment. We observed in D283-MED, D458-MED and MHH-Med1 cells an induction of several DRs

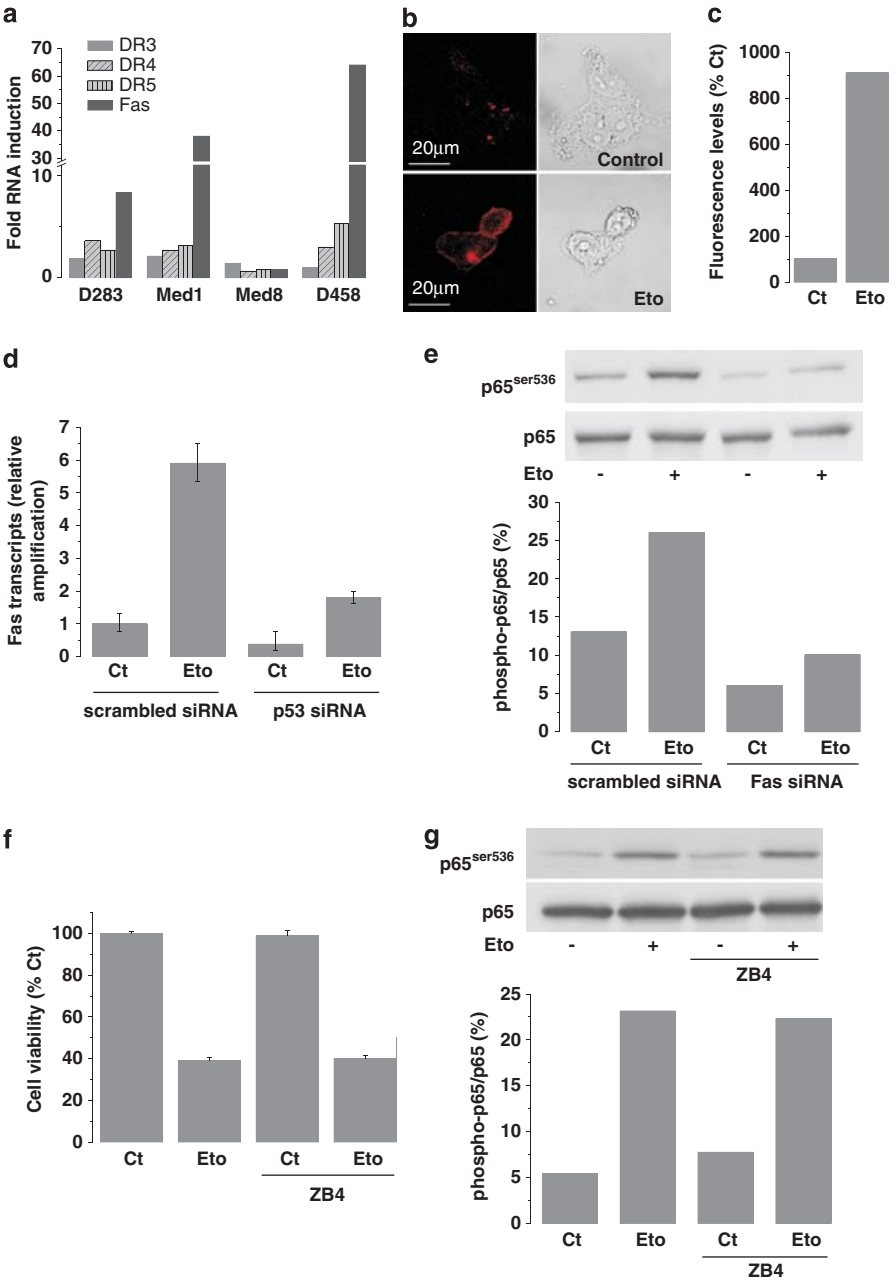

Figure 4 p65 phosphorylation is induced by a p53-dependent death receptors expression. (**a**) Death receptor expression was measured in all cell lines by qPCR upon 8 h etoposide treatment (20 μM). The plot represents the relative quantification compared to control non-treated cells. (**b**) Fas receptor immunocytochemistry on D283-MED cells treated with 20 μM etoposide for 8 h. (**c**) Quantification by flow cytometry of Fas expression to the plasma membrane in D283-MED cells upon 8 h of etoposide treatment (20 μM). (**d**) D283-MED cells were transfected with 100 nM of siRNA directed against p53 or control-scrambled siRNA. After 48 h transfection, cells were treated with etoposide (20 μM, 8 h). Fas mRNA expression was assessed by qPCR. Results are expressed as fold levels induction compared with the control unstimulated cells transfected with scrambled siRNA. Knockdown of p53 was controlled by qPCR (not shown) and western blot (Figure 3c). (**e**) D283-MED cells were transfected with 100 nM siRNA directed against Fas or control-scrambled siRNA. After 48 h transfection, cells were treated with 20 μM etoposide for 6 h and phospho-p65 levels were measured by western blot. The plot represents the quantification of the blot shown. (**f**) D283-MED cells were treated with 20 μM etoposide in the presence or absence of the Fas antagonist ZB4 antibody (5 μg/ml) for 8 h. Cell viability was measured by MTS assay and expressed as % of control untreated cells. (**g**) D283-MED cells were treated for 6 h with etoposide (20 μM) in the presence or absence of the Fas antagonist ZB4 antibody. Phospho-Ser536-p65 levels were evaluated by western blot. The bands were quantified and the phospho-p65/p65 ratio was plotted for the different treatment conditions

mRNA, *DR3*, *DR4*, *DR5* and more strongly *Fas* receptor mRNA (Figure 4a). Conversely, no transcription was induced in MEB-Med8A cells, where the p53 pathway was found to be mutated. The high levels of Fas receptor transcripts were reflected in the expression of the receptor at the plasma membrane in D283-MED and MHH-Med1 cells as measured by immunocytochemistry and flow cytometry (Figure 4b and c and Supplementary Figure S6A). In addition p53

knockdown by siRNA impaired expression of Fas receptor (Figure 4d and Supplementary Figure S6B). We then investigated the role of Fas receptor in p53/p65 crosstalk. D283-MED cells were transfected with a Fas siRNA for 48 h and treated with etoposide for an additional 6 h. Fas receptor knockdown strongly inhibited p65 phosphorylation (Figure 4e). To probe in detail the mechanism of Fas activation, we inhibited the interaction between Fas receptor and its ligand (FasL). However, treatment with the Fas antagonist antibody ZB4 or the inhibitory peptide Kp7-6 did not inhibit etoposide-induced cell death (Figure 4f and Supplementary Figure S7A, B) or p65 phosphorylation (Figure 4g and Supplementary Figure S7C). These results suggested that Fas receptor-induced p65 activation was independent of FasL. This finding was confirmed by the absence of FasL amplification by qPCR (Supplementary Figure S7D) and by the fact that no FasL could be detected by ELISA (not shown). Interestingly, similar observations have been described in other MB cell lines[22] and suggest an important role of receptor oligomerisation in Fas receptor activity.

The upstream role of p53 in cell death sensitivity also takes place in GM cells. To probe the generality of our findings in other central nervous system tumour cells, further experiments were performed in GM cell lines (D566-MG, T98G and U87MG cells). Interestingly, different sensitivities were also observed upon etoposide treatment (Figure 5a), and were again correlated with the activation status of p53 and NF-κB signalling pathways. Indeed, D566-MG and T98G GM cells were found to be unable to accumulate p53 after etoposide treatment (Figure 5b) and consequently no Fas expression (Figure 5c) or p65 phosphorylation (Figure 5b) could be detected. The impairment in p53- and p65-dependent signalling was also confirmed by the absence of induction of specific target genes (mdm2 and IκBα, Figure 5c). These cells were strongly resistant to etoposide-induced cell death as previously observed with the MB MEB-Med8A cells (Figures 2a and 5a). U87MG GM cells showed p53 accumulation (Figure 5b) and Fas transcription (Figure 5c) upon etoposide treatment. However, similarly to the MB MHH-Med1 cells, no p65 activation was detected (Figure 5b

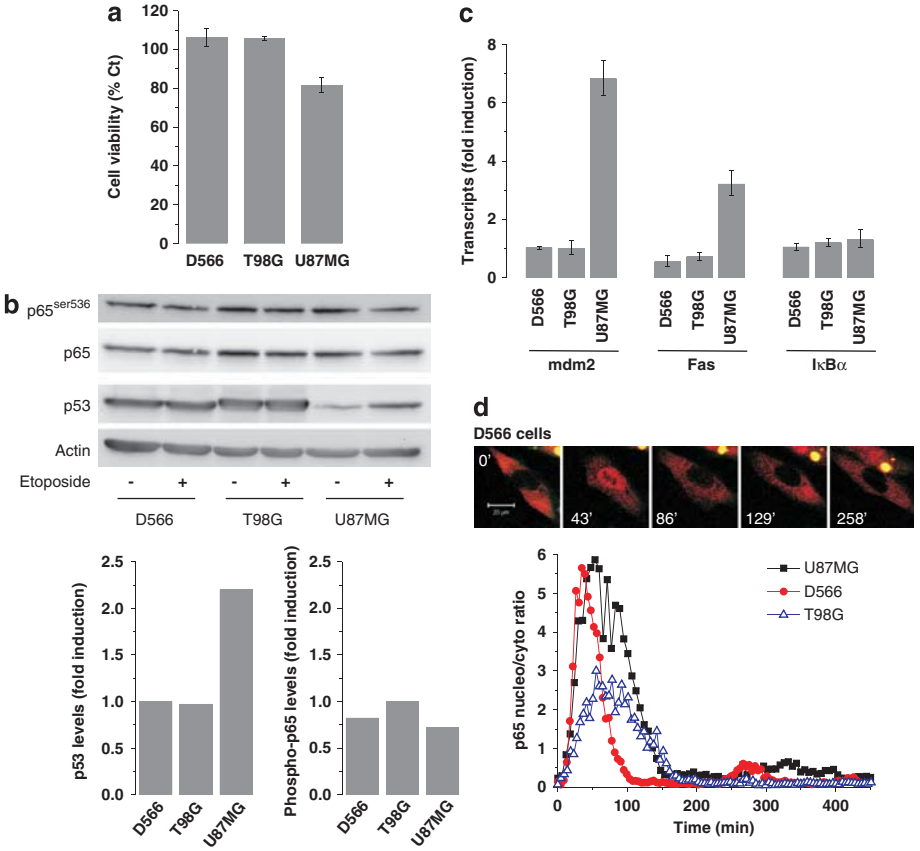

Figure 5 The upstream role of p53 in cell death sensitivity is also valid in glioblastoma cells. (**a**) Cell viability was analysed in several glioblastoma cell lines by MTS assay after 24 h of 20 μM etoposide treatment. (**b**) Glioblastoma cells were treated with 20 μM etoposide for 6 h and p53 expression levels as well as p65 phosphorylation levels were evaluated by western blot in different cell lines. The bands were quantified and the fold induction of phospho-Ser536-p65 (p65 as loading control) and p53 expression (actin as loading control) normalised to the control unstimulated cells were plotted for the different treatment conditions. (**c**) Glioblastoma cells were treated with 20 μM etoposide for 8 h and mRNA level of p53-dependent genes (mdm2 and Fas) and NF-κB-dependent genes (IκBα and A20) were assessed by qPCR. Results are expressed as fold-induction compared with the control unstimulated cells. (**d**) Glioblastoma cells transfected with p65-RedXP and IκBα-EGFP were treated with 10 ng/ml TNFα. Time-lapse confocal microscopy was performed as described in experimental procedures. Mean fluorescence intensities for individual cells were analysed. A typical cell for each cell line was plotted as the p65 nuclear/cytoplasmic ratio as a function of time. Pictures illustrate a typical D566-MG cell at indicated time points. The scale bar represents 20 μm

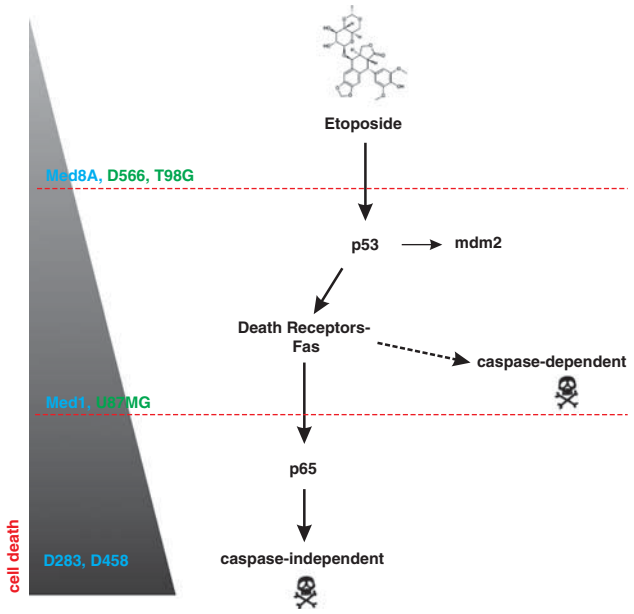

Figure 6 Molecular mechanisms of etoposide-induced cell death in brain tumours. The schematic diagram represents a model of intracellular mechanism induced by etoposide in both GM and MB cells. Depending on the genetic background, cells display different sensitivity to etoposide. Through its genotoxic function, etoposide induces p53 activation. p53 activates the transcription of various genes involved in regulation of cell cycle arrest and cell death as Fas receptor and mdm2. Fas receptor expression at the plasma membrane is able to activate p65 in a FasL-independent manner as well as a caspase-dependent apoptotic cell death. p65 enhances apoptotic death by inducing a caspase-independent cell death. Cells displaying this fully efficient crosstalk are very sensitive to etoposide-induced cell death (D283-MED, D458-MED). Conversely, cells impaired in p53 activation are strongly resistant to cell death (MEB-Med8A, D566-MG, T98G). Interestingly, Cells displaying p53 activity but an impaired p65 activation show intermediate resistance (MHH-Med1, U87MG). MB cell lines are in blue and GM cell lines in green. The grey-to-black gradient illustrates the sensitivity to etoposide-induced cell death. The dotted red lines represent the nods in transduction pathways that are blocked in indicated cell lines

and c) and intermediate cell death sensitivity was observed (Figure 5a). In contrary to the MHH-Med1 cells, the absence of p65 activation in U87MG is not due to an impairment of the NF-κB pathway, as TNFα treatment was able to induce IκBα degradation, p65 phosphorylation and translocation into the nucleus (Figure 5d and Supplementary Figure S8). The two other GM cell lines (D566-MG and T98G) displayed a normal p65 activation and IκBα degradation upon TNFα stimulation similarly to MEB-Med8A cells (Figure 5d and Supplementary Figure S8).

The role of p53, Fas and p65 and the consequences on cell death of mutations at different levels of the signalling cascade in both MB and GM cells are summarised in the diagram Figure 6.

Discussion

Delay in NF-κB induction by etoposide, role of the p65-p53 crosstalk. Our results describe a new mechanism of crosstalk between the p53 and NF-κB signalling pathways through DRs production. This finding may also explain the mechanism by which MB cell lines show differential resistance to etoposide treatment. Previous studies in leukaemia and neuroblastoma cells have described etoposide-induced NF-κB activation.[4,19,23] In those studies NF-κB inhibition was enhancing etoposide-induced apoptosis, whereas we show here a protection of MB cells using three different NF-κB inhibitors acting at different levels of the signalling pathway or by p65 knockdown with siRNA. This role of NF-κB in triggering cell death has previously been observed in osteosarcoma cell line.[12] The difference suggests a tumour-dependent role of p65.

A delayed NF-κB activation has previously been reported using two different stimuli (etoposide and FasL),[19,24] although the mechanism of this delay was not described. The NF-κB activation observed in this study indicates the involvement of IKKα/β and IκBα (Figure 1c) as both BMS-345541 and Bay11-7082 inhibited etoposide-induced p65 phosphorylation. Furthermore, inhibition of either transcription or translation also prevented p65 activation and we have identified p53 and Fas receptor as key upstream proteins. p65-p53 crosstalk has previously been reported. A direct competition with the CBP/p300 proteins,[14–16] whereby p53 down-regulates NF-κB transcription is well documented. This cannot be the case in the system studied here as: (1) p53 inhibition abolished NF-κB activation (Figure 3c and Supplementary Figure S5); and (2) no NF-κB activity could be detected in cells were p53 was defective (MEB-Med8A cells). Bohuslav *et al*.[25] have suggested another mechanism, in which p53 activation is able to induce Ser536 p65 phosphorylation and nuclear translocation through the ribosomal S6 Kinase 1 (Rsk1). This is proposed to be independent of IKK activation and IκBα degradation. We cannot exclude the implication of Rsk1 in our model, yet it is unlikely to be of primary importance as (1) the etoposide-induced p65 phosphorylation is dependent of IKKs activity (Figure 1c), (2) We have observed IκBα degradation following etoposide treatment (not shown) and (3) p65 activation is dependent on a transcriptional event (Figure 1f). This was not the case in the results reported by Bohuslav *et al*.[25]

Etoposide-induced NF-κB activation appeared to be weaker than that from TNFα stimulation as judged by a lower nuclear translocation amplitude and level of phosphorylation[19] (Figure 1d and Supplementary Figure S1A) and indicates that other mechanisms than the ones occurring upon TNFα stimulation are involved. It could be argued that the observed NF-κB activation might in turn modulate p53 activity as a negative feedback loop.[26] This hypothesis was tested by siRNA knockdown of p65 and no change in etoposide-dependent p53 activation was observed (Supplementary Figure S9). However, the cross-regulations between the NF-κB and p53 are likely to be highly complex and dynamic and could also be more subtle and dependent on the stimuli.

Death receptors as a bridge between p53 and NF-κB. It has been previously shown in vascular smooth muscles cells that p53 can induce a rapid expression of Fas to the plasma membrane from the Golgi, without new RNA and protein synthesis.[27] However, we have here observed a

strong induction of the p53-dependent Fas transcription (Figure 4d).

An interesting finding is the involvement of the DR in a ligand-independent manner. We used two different approaches using the specificity of the antagonist antibody ZB4 and the antagonist peptide Kp7-6 (Figure 4f and g and Supplementary Figure S7). We showed no effects of inhibition of Fas–FasL interaction on etoposide-mediated cell death and p65 activation. We therefore checked the presence of FasL expression by ELISA and qPCR. Surprisingly, we did not detect any increase of FasL expression upon etoposide treatment; moreover, we did not detect any basal expression either, compared with two other human cancer cell lines (Supplementary Figure S7D). However, the Fas receptor knockdown by siRNA completely inhibited the etoposide-induced p65 phosphorylation (Figure 4e). Altogether, these results suggest that the strong overexpression of Fas induces a ligand-independent oligomerisation allowing the activation of downstream signalling. It was commonly thought that membranous receptors were in a monomeric form at the membrane, and that oligomerisation was induced by the ligand. However, it has been shown that TNF receptor family members can assemble in a ligand-independent manner to form a preoligomerised complex at the plasma membrane.[28] In addition, more recent work has shown a similar process, in which Fas was able to induce ligand-independent signalling.[29] We have also shown that the overexpression of Fas receptor was sufficient to induce cell death in D283-MED but not in MHH-Med1 cells (Supplementary Figure S10).

Despite few studies describing a caspase-dependent inhibitory effect of Fas on NF-κB,[30,31] it is usually accepted that Fas induces NF-κB.[24,32] This activation involves the adaptor protein FADD, caspase-8 and RIP. Although FADD is likely involved in our signalling cascade, the role of caspase-8 is less clear as caspase-8 inhibition did not inhibit p65 phosphorylation (Supplementary Figure S11). This is in line with the recent study from Neumann *et al.*,[33] who have clearly demonstrated that Fas activates in parallel the caspases (8 and 3) and the NF-κB activity and that blocking the caspases did not impair p65 activation. They have also shown the direct activation of the IKK complex through Fas-associated death domain-like interleukin-1β-converting enzyme-like inhibitory protein (p43-FLIP) formation upon Fas activation, confirming our findings on the role of IKK in etoposide-induced NF-κB activity by Fas recruitment. These results coupled with the role of p65 in MB cell death (Figure 2b and c) support the involvement of a non-apoptotic cell death to enhance efficiently the p53-dependent apoptotic cell death (Figure 3d and e). Interestingly, a non-apoptotic cell death induced by Fas receptor stimulation was previously described.[34] We have observed an induction of autophagy (Supplementary Figure S4) in the presence of etoposide, which could potentially be involved in the Fas-NF-κB-induced cell death.

We have shown by qPCR that etoposide could induce other DRs: DR3, DR4 and DR5 (Figure 4a). As these DR and Fas are members of the TNF receptor family, a part of machinery below these receptors is common and we cannot exclude an additional role of these receptors in NF-κB activation. This is in line with previous reports showing NF-κB activation by different DRs,[35,36] yet in other systems, the role of NF-κB in DRs expression was also described.[37] Moreover, several studies demonstrated that DRs could have a function in chemosensitivity, notably in MB.[38,39] In summary, our results suggest that the DR synthesis and auto-oligomerisation is likely to be involved in activation of the caspase cascade as well as in NF-κB activation. In addition, we cannot exclude the implication of other death domain proteins that could also be involved in the bridge between p53 and NF-κB. For example, p53-induced protein with death domain (PIDD) has been shown to be transactivated by p53 and to activate NF-κB upon DNA damage through sumoylation and ubiquitination of upstream NF-κB modulators.[40]

The integrity of the p53-Fas-NF-κB signalling is required for optimal chemosensitivity of MB cells. We have demonstrated that cells expressing a fully functional connection between p53 and p65 by Fas receptor production are the most sensitive to the DNA-damaging agent etoposide (Figure 6). Indeed, MEB-Med8A, D566-MG and T98G cells that are impaired in p53 signalling are strongly resistant to etoposide. Similar results were described in neuroblastoma.[41] Interestingly, in MHH-Med1 and U87MG cells that bear an apparently normal p53 signalling, but are unable to further activate p65, we observed an intermediate sensitivity (Figures 2a and 5a and model Figure 6). The impairment in p53 signalling in MEB-Med8A cells is at least in part due to the absence of p53wt and the presence of a truncated isoform. This isoform could be p53β according to its molecular weight and migration pattern on western blot.[42] Regarding the MHH-Med1 cells, we have not been able to identify the reason why NF-κB phosphorylation and transcription were completely impaired in these cells even upon the classical TNFα inducer. The cells display a normal expression pattern of p65, IκBα and IKK on a western blot compared with other cell lines (not shown), suggesting a potential mutation upstream in the receptor adaptor molecules.

In conclusion, our study has depicted a new molecular mechanism for etoposide-induced cell death that has clear implications for future clinical treatments. We have shown the importance in determining biomarkers in tumour tissues to adapt the chemotherapeutic treatment in a case-by-case basis. As drug resistance is currently one major problem in chemotherapy, the elucidation of a genomic signature for each tumour should allow bypassing some resistances. Moreover, inducing concomitantly multiple death pathways may also improve considerably the treatment efficiency.

Materials and Methods

Drugs, antibodies and vectors. Protease and phosphatase inhibitor cocktails, PFTα, actynomycin-D, cycloheximide, mouse anti-IgG-Cy3 conjugate and mouse anti-Fas antibody (clone DX2, no. F4424) were from Sigma (St Louis, MO, USA). Etoposide, Wedelolactone, BMS-345541, Bay11-7082, Kp7-6 peptide, tumour necrosis factor-α (TNFα), Fas ligand ELISA kit and mouse anti-actin antibody were from Calbiochem (Darmstadt, Germany). Stealth RNAi siRNAs were from Invitrogen (Carlsbad, CA, USA), and all medium and reagents used in tissue culture were supplied by Gibco Life Technologies (Carlsbad, CA, USA). Fetal calf serum was from Harlan Seralab (Loughborough, UK). Luciferin used for luminometry and luminescence assay was from Biosynth AG (Staad, Switzerland). Mouse anti-p65 (sc-8008) and mouse anti-p53 (sc-263) antibodies

were from Santa Cruz Biotechnology Inc. Rabbit anti-p65/Phospho-Ser536 antibody (no. 3031) was from Cell Signalling (Danvers, MA, USA). BCA protein assay kit and SuperSignal West Dura Extended Duration Chemiluminescent Substrate were from Pierce Biotechnology (Rockford, IL, USA). Mouse anti-CD95 (clone ZB4, no. 05-338) antibody was from Upstate (Billerica, MA, USA). pNF-κB-Luc vector was from Stratagene (Santa Clara, CA, USA). pG-p65-RedXP and pG-IκBα-EGFP were previously described.[4] pCMV-Fas vector was kindly provided by Dr. T Kanda (National Institute of Infectious Diseases, Tokyo, Japan).

Cell lines and culture. D283-MED, T98G and U87MG cells were purchased from ATCC (Manassas, VA, USA) and were maintained in minimal essential medium with Earle's salts supplemented with 10% fetal calf serum, 1% non-essential amino acids and 1 mM sodium pyruvate. D566-MG and D458-MED were kindly provided by Professor DD Bigner (Duke University Medical Center, USA) and were maintained in similar conditions to D283-MED cells. MHH-Med1 cells and MEB-Med8A cells were kindly provided by Professor T Pietsch (University of Bonn, Germany) and were maintained in Dulbecco's modified Eagle medium supplemented with 10% fetal calf serum. Cells were seeded twice per week, and fresh medium was added every 2 days. Cells were grown in a humidified atmosphere of 5% CO2 at 37°C.

Plasmid and siRNA transfection. FuGENE HD (Roche, Basel, Switzerland) was diluted in Opti-MEM medium (Invitrogen) before addition of the plasmid DNA (ratio 8 : 2). After 15 min incubation at RT, the mixture was added on cells in complete medium. For siRNA transfection, HiPerfect (Qiagen, Hilden, Germany) was used instead of FuGENE HD.

Viability assay. Cells were plated in 96-well cell culture plates. Twenty-four hours after plating, cells were treated as indicated for 8–48 h. CellTiter 96 Aqueous One solution (Promega, Madison, WI, USA) was added and was incubated 2 h at 37°C according to the manufacturer's indications. The optical densities were assessed with a plate reader at 492 nm.

Confocal microscopy. Confocal microscopy was carried out on transfected cells in 35 mm glass-bottom dishes (Iwaki, Asahi Techno Glass, Tokyo, Japan) in a humidified CO2 incubator at 37°C, 5% CO2 using a Zeiss LSM510 (Jena, Germany) with a $\times 63$ Plan Apochromatic oil immersion objective (NA = 1.4). EGFP-tagged proteins were excited using an Argon ion laser at 488 nm. Emitted light was detected through a 505–550 nm bandpass filter from a 545 nm dichroic mirror. dsRed fluorescence was excited using a green helium–neon laser (543 nm) and was detected through both a 545 nm dichroic mirror and a 560 nm long-pass filter. Data capture was performed with LSM510 version 3 software (Carl Zeiss GmbH, Jena, Germany) and extraction was carried out with CellTracker v0.6 software (University of Manchester, UK).[43] Nuclear and cytoplasmic integrated fluorescence intensity were determined and the nuclear/cytoplasmic ratio was calculated.

Immunoblotting. Total protein was extracted with a lysis buffer (Tris-HCl pH = 7.5 50 mM, EDTA 1 mM, EGTA 1 mM, Triton X-100 1%, NaF 50 mM, sodium pyrophosphate 5 mM, sodium β-glycerophosphate 10 mM, PMSF 0.1 mM, protease inhibitor cocktail 1/100 and phosphatase inhibitor cocktail 1/100). After 1 h at 4°C on a rotating wheel shaker, the lysates were centrifuged $\geqslant 10\,000 \times g$ for 15 min at 4°C and total protein concentration was measured with BCA assay in the supernatant. A quantity of 40 μg of proteins were resolved by SDS-PAGE (10% gels) and were transferred onto nitrocellulose membrane. The membranes were blocked with 5% nonfat dry milk in TBS-T (Tris-HCl pH = 8 10 mM, NaCl 100 mM, Tween-20 0.1%) and incubated with appropriate primary antibody (overnight, 4°C), followed by incubation with horseradish peroxidase-conjugated secondary antibody (1 h, RT). SuperSignal West Dura Extended Duration Chemiluminescent Substrate was used for ECL reaction and the signal was detected and quantified using G:box gel doc system (Syngene, Cambridge, UK).

Luminometry. Cells were transfected with a firefly luciferase reporter construct containing five repeats of the NF-κB-binding site (pNF-Luc). Twenty-four hours later, cells were treated as indicated. Cell lysis and luminescence measurements were performed as described previously[4] using a PerkinElmer EnVision plate reader (Waltham, MA, USA).

Caspase activity. Cells were plated in 96-well white plates. Caspase-Glo 8 and 3/7 kits (Promega) were used following the manufacturer's instructions.

Luminescence microscopy. Real-time luminescence imaging was performed 24 h after transfection of cells in 35 mm glass-base dishes. Luciferin (0.5 μM) was added in the culture medium 2 h before drug treatment. Luminescence imaging was carried out in a humidified incubator (37°C, 5% CO2) using a Hamamatsu VIM photon counting camera attached to a Zeiss Axiovert 135 TV with a $\times 20$ FLUAR objective. Argus-20 control program version 3.53 software (Hamamatsu Photonics, Hamamatsu City, Japan) was used for image acquisition, AQM Advance 6.0 software (Kinetic Imaging, Nottingham, UK) was used for image analysis. Images were acquired using 30 min integration time.

Immunocytochemistry. Cells plated in 35 mm glass-base dishes were fixed with paraformaldehyde 4% for 15 min at room temperature and treated with NH4Cl 50 mM for 20 min at RT. After blocking in PBS – 1% BSA – 0.1% Triton X-100 for 20 min, cells were incubated with anti-Fas antibody (1 : 500) in blocking buffer for 1 h. After three washes, cells were incubated with an anti-mouse IgG Cy3 conjugate (1 : 500) for 30 min. Cells were imaged using a Zeiss LSM 510 confocal microscope.

Quantitative RT-PCR. Cellular RNAs were purified using Qiagen RNeasy mini kit according to the manufacturer's instructions. cDNA were synthetised with QuantiTect Reverse Transcription Kit (Qiagen) and qPCR were performed using ABI Power SYBR Green PCR master mix (Carlsbad, CA, USA) according the manufacturer's instructions. We used an ABI 7500 Fast Real-Time PCR System. Cyclophilin A was used as a calibrator for the relative amplification of genes of interest calculations.

Primer sequences are as follows: Cyclophilin A forward: GCTTTGGGTCCAG GAATGG; Cyclophilin A reverse: GTTGTCCACAGTCAGCAATGGT; p65 forward: AGCGCATCCAGACCAACAA; p65 reverse: TAGTCCCCACGCTGCTCTTC; p53 forward: GGCCCACTTCACCGTACTAA; p53 reverse: GTGGTTTCAAGGCCA GATGT; mdm2 forward: GGTGGGAGTGATCAAAAGGA; mdm2 reverse: ACACA GAGCCAGGCTTTCAT; DR3 forward: CACCCTTCTAGCACCTCCTG; DR3 reverse: CCAGCTGTTACCCACCAACT; DR4 forward: GCTGCAACCATCAAACTT CA; DR4 reverse: GGCTATGTTCCCATTGCTGT; DR5 forward: TGCTCTGAT CACCCAACAAG; DR5 reverse: CAGGTGGACACAATCCCTCT; Fas forward: GCATCTGGACCCTCCTACCT; Fas reverse: CAGGGCTTATGGCAGAATTG; IκBα forward: TGGTGTCCTTGGGTGCTGAT; IκBα reverse: . GGCAGTCCGGC CATTACA; A20 forward: AACGGTGACGGCAATTGC; A20 reverse: TGAA CGCCCCACATGTACTG.

Statistical analysis. Histograms represent the mean values ± S.E.M. Statistical significance was determined by one-way ANOVA followed by a Bonferroni multiple comparison test. Difference was considered as significant at $P < 0.01$. All these experiments were performed at least three times.

Conflict of interest

The authors declare no conflict of interest.

Acknowledgements. We thank Samantha Dickson Brain Tumour Trust (SDBTT 15/37) and BBSRC for funding this work. VS is a recipient of a BBSRC David Phillips fellowship (BBC5204711). We thank Professor T Pietsch and Professor DD Bigner for providing MB and GM cell lines. We also thank Dr. T Kanda for providing the CMV-Fas vector.

Author contribution: DM designed and performed the experiments and analysed the results. DS trained DM in confocal microscopy, immunocytochemistry and performed the flow cytometry experiments. DS was also involved in discussion about analysis and interpretation of the results. MW provided expert advice and guidance throughout this study. HMcD and BP brought their medical expertise in the elaboration of the project. VS elaborated the project and supervised the design and analysis of the experiments. DM and VS wrote the article.

1. Pizer B, Clifford S. Medulloblastoma: new insights into biology and treatment. *Arch Dis Child* 2008; **93**: 137–144.
2. Rutkowski S. Current treatment approaches to early childhood medulloblastoma. *Expert Review of Neurotherapeutics* 2006; **6**: 1211–1221.
3. Campbell KJ, Rocha S, Perkins ND. Active repression of antiapoptotic gene expression by RelA(p65) NF-kappa B. *Mol Cell* 2004; **13**: 853–865.

4. Nelson DE, Ihekwaba AE, Elliott M, Johnson JR, Gibney CA, Foreman BE *et al.* Oscillations in NF-kappaB signaling control the dynamics of gene expression. *Science* 2004; **306**: 704–708.
5. Fritsche M, Haessler C, Brandner G. Induction of nuclear accumulation of the tumor-suppressor protein p53 by DNA-damaging agents. *Oncogene* 1993; **8**: 307–318.
6. Muller M, Wilder S, Bannasch D, Israeli D, Lehlbach K, Li-Weber M *et al.* p53 activates the CD95 (APO-1/Fas) gene in response to DNA damage by anticancer drugs. *J Exp Med* 1998; **188**: 2033–2045.
7. Vallabhapurapu S, Karin M. Regulation and function of NF-kappaB transcription factors in the immune system. *Annu Rev Immunol* 2009; **27**: 693–733.
8. See V, Rajala NK, Spiller DG, White MR. Calcium-dependent regulation of the cell cycle via a novel MAPK–NF-kappaB pathway in Swiss 3T3 cells. *J Cell Biol* 2004; **166**: 661–672.
9. Karin M. Nuclear factor-kappaB in cancer development and progression. *Nature* 2006; **441**: 431–436.
10. Perkins ND. NF-kappaB: tumor promoter or suppressor? *Trends Cell Biol* 2004; **14**: 64–69.
11. Bian X, McAllister-Lucas LM, Shao F, Schumacher KR, Feng Z, Porter AG *et al.* NF-kappa B activation mediates doxorubicin-induced cell death in N-type neuroblastoma cells. *J Biol Chem* 2001; **276**: 48921–48929.
12. Ryan KM, Ernst MK, Rice NR, Vousden KH. Role of NF-kappaB in p53-mediated programmed cell death. *Nature* 2000; **404**: 892–897.
13. Spurgers KB, Gold DL, Coombes KR, Bohnenstiehl NL, Mullins B, Meyn RE *et al.* Identification of cell cycle regulatory genes as principal targets of p53-mediated transcriptional repression. *J Biol Chem* 2006; **281**: 25134–25142.
14. Huang WC, Ju TK, Hung MC, Chen CC. Phosphorylation of CBP by IKKalpha promotes cell growth by switching the binding preference of CBP from p53 to NF-kappaB. *Mol Cell* 2007; **26**: 75–87.
15. Ravi R, Mookerjee B, van Hensbergen Y, Bedi GC, Giordano A, El-Deiry WS *et al.* p53-mediated repression of nuclear factor-kappaB RelA via the transcriptional integrator p300. *Cancer Res* 1998; **58**: 4531–4536.
16. Webster GA, Perkins ND. Transcriptional cross talk between NF-kappaB and p53. *Mol Cell Biol* 1999; **19**: 3485–3495.
17. Schumm K, Rocha S, Caamano J, Perkins ND. Regulation of p53 tumour suppressor target gene expression by the p52 NF-kappaB subunit. *EMBO J* 2006; **25**: 4820–4832.
18. Chinnaiyan AM, O'Rourke K, Tewari M, Dixit VM. FADD, a novel death domain-containing protein, interacts with the death domain of Fas and initiates apoptosis. *Cell* 1995; **81**: 505–512.
19. Morotti A, Cilloni D, Pautasso M, Messa F, Arruga F, Defilippi I *et al.* NF-kB inhibition as a strategy to enhance etoposide-induced apoptosis in K562 cell line. *Am J Hematol* 2006; **81**: 938–945.
20. Ashall L, Horton CA, Nelson DE, Paszek P, Harper CV, Sillitoe K *et al.* Pulsatile stimulation determines timing and specificity of NF-kappaB-dependent transcription. *Science* 2009; **324**: 242–246.
21. Nam C, Yamauchi H, Nakayama H, Doi K. Etoposide induces apoptosis and cell cycle arrest of neuroepithelial cells in a p53-related manner. *Neurotoxicol Teratol* 2006; **28**: 664–672.
22. Wang Q, Li H, Wang X-W, Wu D-c, Chen X-Y, Liu J. Resveratrol promotes differentiation and induces Fas-independent apoptosis of human medulloblastoma cells. *Neurosci Lett* 2003; **351**: 83–86.
23. Armstrong MB, Bian X, Liu Y, Subramanian C, Ratanaproeksa AB, Shao F *et al.* Signaling from p53 to NF-kappaB determines the chemotherapy responsiveness of neuroblastoma. *Neoplasia (New York, NY)* 2006; **8**: 967–977.
24. Imamura R, Konaka K, Matsumoto N, Hasegawa M, Fukui M, Mukaida N *et al.* Fas ligand induces cell-autonomous NF-kappaB activation and interleukin-8 production by a mechanism distinct from that of tumor necrosis factor-alpha. *J Biol Chem* 2004; **279**: 46415–46423.
25. Bohuslav J, Chen L-F, Kwon H, Mu Y, Greene WC. p53 induces NF-κB activation by an IκB kinase-independent mechanism involving phosphorylation of p65 by ribosomal S6 kinase 1. *J Biol Chem* 2004; **279**: 26115–26125.
26. Tergaonkar V, Pando M, Vafa O, Wahl G, Verma I. p53 stabilization is decreased upon NFkappaB activation: a role for NFkappaB in acquisition of resistance to chemotherapy. *Cancer Cell* 2002; **1**: 493–503.
27. Bennett M, Macdonald K, Chan SW, Luzio JP, Simari R, Weissberg P. Cell surface trafficking of Fas: a rapid mechanism of p53-mediated apoptosis. *Science* 1998; **282**: 290–293.
28. Papoff G, Hausler P, Eramo A, Pagano MG, Di Leve G, Signore A *et al.* Identification and characterization of a ligand-independent oligomerization domain in the extracellular region of the CD95 death receptor. *J Biol Chem* 1999; **274**: 38241–38250.
29. Li S, Zhou Y, Dong Y, Ip C. Doxorubicin and selenium cooperatively induce fas signaling in the absence of Fas/Fas ligand interaction. *Anticancer Res* 2007; **27** (5A): 3075–3082.
30. Wong HK, Tsokos GC. Fas (CD95) ligation inhibits activation of NF-kappa B by targeting p65-Rel A in a caspase-dependent manner. *Clin Immunol (Orlando, Fla)* 2006; **121**: 47–53.
31. Ravi R, Bedi A, Fuchs EJ, Bedi A. CD95 (Fas)-induced caspase-mediated proteolysis of NF-kappaB. *Cancer Res* 1998; **58**: 882–886.
32. Kreuz S, Siegmund D, Rumpf JJ, Samel D, Leverkus M, Janssen O *et al.* NFkappaB activation by Fas is mediated through FADD, caspase-8, and RIP and is inhibited by FLIP. *J Cell Biol* 2004; **166**: 369–380.
33. Neumann L, Pforr C, Beaudouin J, Pappa A, Fricker N, Krammer PH *et al.* Dynamics within the CD95 death-inducing signaling complex decide life and death of cells. *Mol Syst Biol* 2010; **6**: 352.
34. Holler N, Zaru R, Micheau O, Thome M, Attinger A, Valitutti S *et al.* Fas triggers an alternative, caspase-8-independent cell death pathway using the kinase RIP as effector molecule. *Nat Immunol* 2000; **1**: 489–495.
35. Schneider P, Thome M, Burns K, Bodmer JL, Hofmann K, Kataoka T *et al.* TRAIL receptors 1 (DR4) and 2 (DR5) signal FADD-dependent apoptosis and activate NF-kappaB. *Immunity* 1997; **7**: 831–836.
36. Chinnaiyan AM, O'Rourke K, Yu GL, Lyons RH, Garg M, Duan DR *et al.* Signal transduction by DR3, a death domain-containing receptor related to TNFR-1 and CD95. *Science* 1996; **274**: 990–992.
37. Shetty S, Gladden JB, Henson ES, Hu X, Villanueva J, Haney N *et al.* Tumor necrosis factor-related apoptosis inducing ligand (TRAIL) up-regulates death receptor 5 (DR5) mediated by NFkappaB activation in epithelial derived cell lines. *Apoptosis* 2002; **7**: 413–420.
38. Aguilera DG, Das CM, Sinnappah-Kang ND, Joyce C, Taylor PH, Wen S *et al.* Reactivation of death receptor 4 (DR4) expression sensitizes medulloblastoma cell lines to TRAIL. *J Neurooncol* 2009; **93**: 303–318.
39. Lam V, Findley HW, Reed JC, Freedman MH, Goldenberg GJ. Comparison of DR5 and Fas expression levels relative to the chemosensitivity of acute lymphoblastic leukemia cell lines. *Leukemia Res* 2002; **26**: 503–513.
40. Tinel A, Janssens S, Lippens S, Cuenin S, Logette E, Jaccard B *et al.* Autoproteolysis of PIDD marks the bifurcation between pro-death caspase-2 and pro-survival NF-kappaB pathway. *EMBO J* 2007; **26**: 197–208.
41. Keshelava N, Zuo JJ, Chen P, Waidyaratne SN, Luna MC, Gomer CJ *et al.* Loss of p53 function confers high-level multidrug resistance in neuroblastoma cell lines. *Cancer Res* 2001; **61**: 6185–6193.
42. Bourdon JC. p53 Family isoforms. *Curr Pharm Biotechnol* 2007; **8**: 332–336.
43. Shen H, Nelson G, Nelson DE, Kennedy S, Spiller DG, Griffiths T *et al.* Automated tracking of gene expression in individual cells and cell compartments. *J Royal Soc, Interface/the Royal Society* 2006; **3**: 787–794.

Supplementary Information accompanies the paper on Cell Death and Disease website (http://www.nature.com/cddis)